A Threshold Method for Robust and Fast Estimation of Land-Surface Phenology Using Google Earth Engine

Adrià Descals, Aleixandre Verger, Gaofei Yin, and Josep Peñuelas

***Abstract*—Cloud-based platforms are changing the way of analyzing remotely sensed data by providing high computational power and rapid access to massive volumes of data. Several types of studies use cloud-based platforms for global-scale analyses, but the number of land-surface phenology (LSP) studies that use cloud-based platforms is low. We analyzed the performance of the state-of-the-art LSP algorithms and propose a new threshold-based method that we implemented in Google Earth Engine (GEE). This new LSP method, called maximum separation (MS) method, applies a moving window that estimates the ratio of observations that exceed a given threshold before and after the central day. The start and end of the growing season are the days of the year when the difference between the ratios before and after the central day are minimal and maximal. The MODIS phenology metrics estimated with the MS method showed similar performances as traditional threshold methods when compared with ground estimations derived from the PhenoCam dataset, a network of digital cameras that provides near-surface remotely sensed observations of vegetation phenology. The main advantage of the MS method is that it can be directly applied to daily nonsmoothed time series without any additional preprocessing steps. The implementation of the proposed method in GEE allowed the processing of global phenological maps derived from MODIS. The distribution of code in GEE allows the reproducibility of results and the rapid processing of LSP metrics by the scientific community.**

***Index Terms*—Cloud computing, global monitoring, Google Earth Engine (GEE), land surface phenology (LSP), threshold method.**

I. Introduction

THE study of land-surface phenology (LSP) entails the estimation of metrics from remotely sensed vegetation seasonality [1]. Its study is important for reliably estimating vegetation dynamics, commonly the start and end of the growing season (SoS and EoS), which correspond to the timing of the year when the vegetation is released from dormancy and when the growing season ends. Phenology has recently gained importance because of its linkage with global warming. Several studies have found that the length of the growing season has increased in recent decades due to the global warming [2], [3]. The influence of the temperature and other climatic factors on the vegetation dynamics is still under discussion [4], [5], and reliable estimates of phenological metrics at a global scale are required to understand the links between the climatic factors and vegetation phenology.

Many cloud-based platforms have recently become available to the scientific community, which has allowed the processing of large amounts of remotely sensed data. Google Earth Engine (GEE) is one of the most popular platforms [6]. Some studies have addressed temporal aspects such as data smoothing and, particularly, phenology estimation using a curve fitting method [7], but the number of LSP studies that make use of cloud-computing platforms is still low. One reason that explains the low number of LSP studies is that temporal processing in cloud platforms requires methods that can be vectorized and easily implemented. Code vectorization is the process of transforming an algorithm so that instead of processing elements on an array separately, generally with a *for* loop, the operations are performed on all components of the array simultaneously [8]. Such elements of the array are commonly pixel values or satellite time series. Code vectorization enhances the computational power of GEE and allows the processing of satellite time series in an optimized manner. A freely available implementation of an LSP method in GEE would allow the fast processing of satellite archives in a variety of products and would ease the accessibility of data for computing large-scale LSP maps at different spatial resolutions.

The results of the state-of-the-art LSP methods, however, are affected to some extent by noise, gaps, and outliers presented in the time series, so a set of preprocessing steps is required to prepare and reconstruct the time series captured from remotely sensed data [1]. These steps commonly include outlier rejection filters, temporal compositing, smoothing, gap-filling, and interpolation of the time series to regular or daily time steps. A commonly used approach in the literature is the maximum value composite [9], [10]. This temporal compositing method computes the maximum value of the vegetation index for a temporal window and assumes that negatively biased values are contaminated by clouds or cloud shadows. In addition to the temporal compositing, smoothing techniques are also used to reduce the noise of the time series. The most common smoothing techniques can be classified into moving-window [11]–[13] and

Manuscript received August 21, 2020; revised October 23, 2020; accepted November 11, 2020. Date of publication November 20, 2020; date of current version January 6, 2021. This work was supported in part by the European Research Council ERC SyG-610028 2013-Synergy-Grant, IMBALANCE-P, in part by the Marie Skłodowska-Curie Grant of European Union's Horizon 2020 Research and Innovation Programme under Grant 835541, in part by the Spanish Project CGL2016-79835-P, in part by the Ministry of Science and Innovation of Spain FPI under Grant BES—2017-080197, and in part by the Catalan under Grant SGR 2017-1005. *(Corresponding author: Adrià Descals.)*

The authors are with the Centre de Recerca Ecològica i Aplicacions Forestals, 08193 Barcelona, Spain (e-mail: adriadescals@gmail.com; verger@creaf.uab.cat; g.yin@creaf.uab.cat; josep.Penuelas@uab.cat).

This article has supplementary downloadable material available at https://doi.org/10.1109/JSTARS.2020.3039554, provided by the authors.

Digital Object Identifier 10.1109/JSTARS.2020.3039554

curve-fitting methods [9], [10], [14], [15]. The first category runs a moving window in the time series, such as the moving average filter, while the second category fits a function to the time series, such as logistic and Gaussian models. These preprocessing steps have various shortcomings.

1) They are highly parametric (window size, smoothing type), and results are not robust in all regions; preprocessing may work well in some places but not others.
2) Smoothing may affect the temporal pattern of vegetation seasonality and may, thus, add a bias to the LSP estimations.
3) Defining the smoothing functions and their parameters requires expert knowledge and makes their implementation time consuming, although some program packages, such as SPIRITS [16] and TIMESAT [17], include well-implemented methods.

The choice of the preprocessing steps is critical, because the robustness of the results of LSP methods greatly depends on their quality [1]. The complexity of these preprocessing steps also impedes the implementation of LSP methods in GEE. The aim of this study was to develop a variant of the threshold method that, first, does not require preprocessing steps and, thus, does not need excessive user-defined parameters, second, has fast computing time and can be easily implemented in cloud-processing platforms, third, can be directly applied to daily remotely sensed observations and still compares well with LSP metrics estimated with ground data.

II. Data and Methods

A. LSP Extraction Methods

1) Maximum Separation Method: The method we propose, which we named maximum separation (MS) method, is a variant of the threshold method. Given a time series of paired values *{t, b}*, where *t* is the time in days and *b* is the vegetation activity represented by a biophysical variable, a vegetation index, a reflectance band, or any measure of greenness [see Fig. 1(a)], we defined a threshold value *u* dynamically [18] with (1). The threshold is dynamic because it is determined by a percentage (p) of the amplitude (difference between the minimum ($b_{\min}$) and maximum ($b_{\max}$) values of the season).

$$u = (b_{\max} - b_{\min})p + b_{\min}. \tag{1}$$

The threshold u is used to classify binarily the time series into 0, when $b < u$, and 1, when $b > u$. The binary time series b' [see Fig. 1(b)] has values equal to zero during the dormant period and values equal to one during the growing season. The method then runs a moving window operation for each day of the binary time series. The operation calculates the difference between the proportion of observations with vegetation activity ($b' = 1$) before and after the central day of the moving window as follows:

$$d = \sum {b'_{\text{before}}}/{n_{before}} - \sum {b'_{after}}/{n_{after}} \tag{2}$$

where n_{before} and n_{after} are the total number of observations before and after the central day of the moving window, and

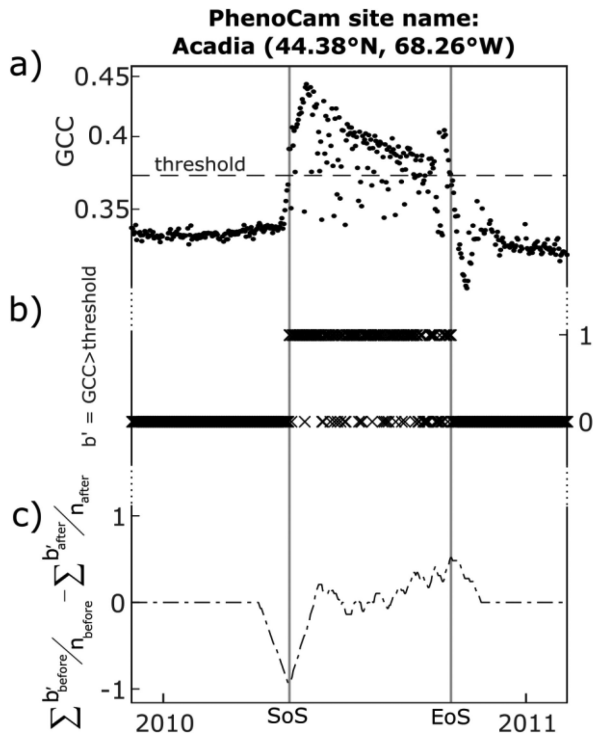

Fig. 1. Estimation of the start of season (SoS) and end of season (EoS) using Maximum Separation (MS) method at the Acadia PhenoCam deciduous forest site in 2010. a) Time series of Green Chromatic Coordinate Index (GCC). b) Binary classification of the time series (0 = dormant period, 1 = growing season). c) Time series obtained by applying a moving window that estimates the difference in the proportion of growing season observations before and after a given day. SoS and EoS correspond to the minimum and maximum values in c), respectively. We used a dynamic threshold of 50% of the amplitude. The semiperiod of the moving window when calculating the proportions is 30 days.

b'_{before} and b'_{after} are the number of observations above the threshold before and after the central day.

The moving window generates a new time series $\{t, d\}$, with minimal values close to –1 when the time series exceeds the threshold and maximal values close to 1 at the end of the season [see Fig. 1(c)]. SoS (t_{sos}) corresponds to the day when d is lowest, and EoS (t_{eos}) corresponds to the day when d is highest. We named the method MS since the SoS and EoS represent the days when the difference between observations above the threshold before and after these dates is maximal.

The running window in (2) can be applied to the entire time series and, then, the minimum and maximum ratios can be searched within a natural year (e.g., from 1 January to 31 December) or, in case of double seasonality, within a specific range of months. This property simplifies the LSP estimation in the Southern Hemisphere, where the main growing season usually occurs from November to February.

2) Threshold Method: The threshold method assigns the SoS (t_{sos}) to the first day when the seasonal time series b exceeds a threshold u after the dormant period, while EoS (t_{eos}) is the last day of the season when b is greater than the threshold u. The threshold is computed dynamically with (1). The threshold method is inherently affected by noise in the time series and, thus, smoothing techniques are required before its application [1]. Here, we used three preprocessing methods.

1) The first preprocessing method (TH1) used a variant of the so-called maximum composite value [19]. The maximum composite value estimates the maximum value of a moving window. We used the 80th percentile instead, which was more robust against outliers. We estimated the composite every eight days. The snow observations were replaced with the 5th percentile value obtained from the entire snow-free time series. This reclassification aims to reduce the sharp increase in the vegetation indices, particularly in NDVI, during the transition from snow to snow-free period, which may lead to unreliable estimate of the SoS. This approach has been adopted for LSP estimation in high-latitude biomes [15] and at the global scale [20]. Finally, we applied a linear interpolation to convert the composite time series to daily estimates.
2) The second preprocessing method (TH2) involved an outlier rejection algorithm that excluded low values, a smoothing step with the Savitzky–Golay filter [21], and a linear interpolation. The outlier rejection excluded observations that exceeded a level of tolerance to adjacent observations. The tolerance was 0.2 times the interpolated value for the given observation. The snow-contaminated values were replaced with the fifth value of the snow-free time series and the cloud-contaminated values were filled by a linear interpolation. The Savitzky–Golay filter was then applied with a second polynomial order and a frame length of 21 days. The parameters of the Savitzky–Golay filter were set by trial and error (see an example of the compositing in Fig. 1 in the supplementary material). These parameters have a strong influence in the reconstruction of the time series.
3) The last preprocessing method (TH3) was a curve-fitting method. We fitted a logistic function, in the following equation to the first half of the season and another to the second half:

$$f(t; a, b, c) = \frac{b}{1 + e^{-a(t-c)}} \tag{3}$$

where t is the day of the year; a, b, and c are the parameters to be fitted: a determines the steepness of the curve, b is the maximum value of the time series, and c represents the maximum increase or decrease in the time series and is commonly associated with the SoS and EoS. We used the curve fitting only as a smoothing step, and the phenological metrics were extracted using the threshold method over the fitted function.

B. Data

1) MODIS Data: We extracted the phenology metrics SoS and EoS to the following MODIS products. First, the MCD15A3H leaf area index (LAI) product [22], which has a temporal resolution of four days at 500 m of spatial resolution. Second, the daily MOD09GA product [23], also at 500 m, from which we estimated the NDVI, the EVI, and the GCC Index. The MOD09GA data are available from the year 2000, while MCD15A3H from 2002. The NDVI, EVI, and LAI are among the most commonly used vegetation indices in phenology studies [1], while GCC is a vegetation index available in the PhenoCam dataset that has recently taken relevance in phenology studies because it is invariant to cloud shadows [24]. The NDVI, EVI, and GCC are estimated directly from the spectral bands (see Table 1 of the supplementary material) and reflect the amount of live green vegetation in a pixel. These indices correlate with LAI, which is a biophysical variable that indicates the one-side green leaf area per pixel (m^2m^{-2}). The LAI product in MCD15A3H product is estimated from modeled radiances [25].

2) PhenoCam Dataset: The LSP metrics estimated with the MODIS products were validated with the PhenoCam Dataset v2.0 [26]. PhenoCam is a network of digital cameras that records images of the vegetation at a high temporal resolution (commonly 30 min), at a close range, and for a diverse range of ecosystems. The time series of images recorded by the digital cameras provide information on the seasonal changes in vegetation greenness that can be used to validate the phenology metrics extracted from remotely sensed satellite data. PhenoCam has been previously used for validation LSP estimated from MODIS data [27], VEGETATION and PROBA-V [12], and Landsat-8 and Sentinel-2 [28].

We considered all the sites of the PhenoCam dataset, but rejected the sites that presented continuous gaps in the time series (with gaps $>$30 days) or years with missing data. A total of 212 sites were considered in the study; 9 sites in evergreen needleleaf forests (ENF), 23 sites in deciduous broadleaf forests (DBF), 77 sites in mixed forests (MX), 7 sites in open shrublands (OSH), 6 sites in woody savannah (OSH), 3 sites in savannah (SAV), 23 sites in grasslands (GRA), 48 sites in temporary crops (CRO1), and 16 sites in cropland/natural vegetation mosaics (CRO2) (see Table 2, of the supplementary material, for more metadata information of the PhenoCam sites and location map in Fig. 2 of the supplementary material). Sites that presented time series with consistent gaps were rejected from the analysis.

PhenoCam Dataset v2.0 provides not only near-surface images but also the GCC-generated time series for certain areas of the image. The different regions observed by the digital camera may cover different types of vegetation that are presented in the site. We used the GCC time series of the primary vegetation type when more than one vegetation type was present in the PhenoCam site. The time coverage of PhenoCam data depends on the date when the digital camera was installed and, therefore, differs from one site to another; the PhenoCam that provided the earliest data was for year 2001, and the latest images were taken in 2018. The temporal coverage of the PhenoCam sites overlaps with the MODIS time series; 2000–2020 for MOD09GA and 2002–2020 for MCD15A3H.

C. Experimental Setup

The phenology metrics, SoS and EoS, estimated with MODIS GCC, NDVI, EVI, and LAI were compared with the same metrics estimated with the GCC time series in the PhenoCam network. We reported the comparison between the satellite and the near-surface estimates in terms of the mean error (ME) and root-mean-squared error (RMSE) (see formulas in Table 3 of the supplementary material). The ME represents a measure of the bias (mean average of the LSP differences PhenoCam—MODIS: positive ME indicates higher PhenoCam values than MODIS) and the RMSE gives an indication of the accuracy of the MODIS in relation to the PhenoCam LSP estimations (the standard deviation of an average MODIS LST estimation

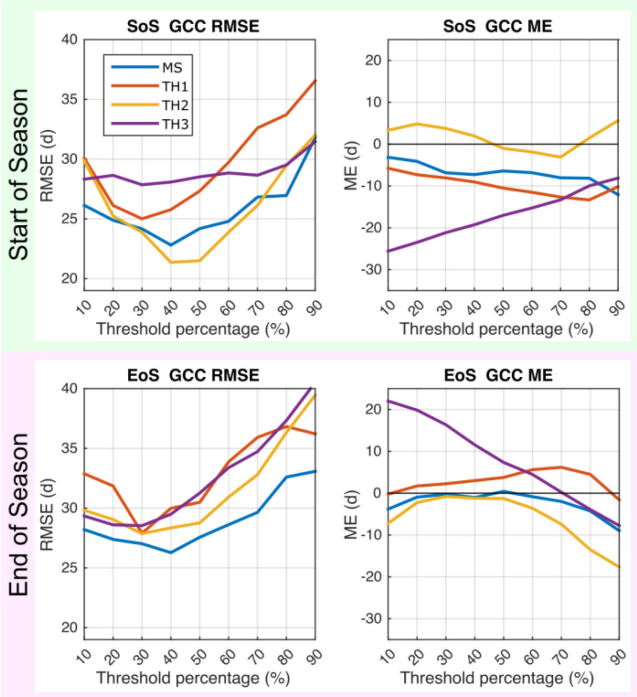

Fig. 2. Root mean square error (RMSE) and mean errror (ME) obtained from the comparison of the land surface phenology (LSP) metrics generated with MODIS Green Chromatic Coordinate Index (GCC) and the PhenoCam dataset for a range of threshold values. The LSP metrics are the start of season (SoS) and end of season (EoS).

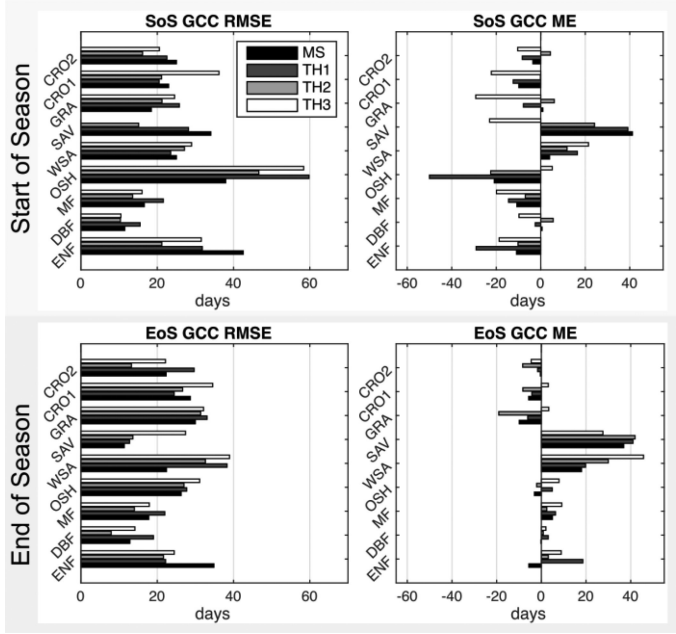

Fig. 3. Root mean square error (RMSE) and mean errror (ME) obtained from the comparison of the land surface phenology (LSP) metrics generated with MODIS GCC and the PhenoCam dataset. The comparison is based on the land cover of the Phenocam sites: evergreen needleleaf forests (ENF), deciduous broadleaf forests (DBF), mixed forests (MX), open shrublands (OSH), woody savannah (OSH), savannah (SAV), grasslands (GRA), temporary crops (CRO1), and cropland/natural vegetation mosaics (CRO2). The LSP metrics are the Start (SoS) and the End of Season (EoS).

from the PhenoCam LSP estimation). The comparison between MODIS and PhenoCam LSP metrics aimed to test the performance of the MS in comparison to the three variants of the threshold method based on two aspects: 1) threshold percentage [variable p in (1)]. We estimated the SoS and EoS with p values ranging from 10% to 90% in steps of 10%. 2) Primary vegetation type of the Phenocam site. For this case, we reported the ME and RMSE only for a threshold percentage of 50%.

We also tested the influence of the window size but, since we found that this parameter has a marginal effect when it takes large values, we set the window radius to 30 days in all experiments of the study. A window size of 30 days represents a good compromise between robustness of the method against noise and computing time.

Finally, we used GEE to generate maps of the SoS and EoS from the MODIS variables: GCC, NDVI, EVI, and LAI. The phenological maps in GEE were generated with the MS method with a threshold percentage of 50% and a window radius of 30 days. We used the RESOLVE Ecoregions 2017 map [29] in order to mask the biomes that show a negligible seasonality in the selected MODIS variables. The masked biomes were the tropical and subtropical dry broadleaf forests, tropical and subtropical coniferous forests, deserts and xeric shrublands, and mangroves.

III. Results

The size of the moving window and the threshold percentage are the only parameters used in MS. Fig. 3 of the supplementary material shows the smoothing effect of the window size (semiperiod of 10, 30, and 90 days) over a time series of daily MODIS GCC (see Fig. 3(a) of the supplementary material) for the Acadia site in the PhenoCam network. The smoothing in the time series derived from (2) is more remarkable in high window sizes (see Fig. 3(c) and 3d of the supplementary material), and the absolute maximum and minimum, corresponding to the phenology metrics, are well-defined in the time series. A window size of ten days, however, does not capture the maximum difference between dormant and growth observation (see Fig. 3(b) of the supplementary material), which in turn results in unrealistic LSP estimations.

The MS showed similar results as the best threshold method, which was TH2, for all MODIS variables (see Fig. 4 of the supplementary material and Fig. 2). TH2 showed the best results for the SoS, while the MS showed better results for the EoS, although overall differences between LSP methods were marginal and none of the MODIS variables excelled in the comparison with PhenoCam. The best result in terms of RMSE was obtained with a threshold percentage of 40% (SoS RMSE = 19.8 d in TH2 using NDVI; EoS RMSE = 23.0 d in MS using LAI). Threshold percentages that ranged from 30% to 60% showed the best results in terms of RMSE for GCC, NDVI, EVI, and LAI, and low accuracy in extreme percentages, particularly >80%. The SoS showed better results than the EoS; the minimum RMSE ranged from 20 to 25 days in the SoS, while the same statistic was between 25 and 30 days in the EoS for the GCC, NDVI, and EVI. The impact of the threshold was less significant in terms of ME for the SoS, but more apparent in the EoS. TH2 outperformed in SoS with a negligible bias for all variables. MS, TH1, and TH2 showed a similar pattern in the ME regarding the threshold percentage, while the TH3 (logistic fitting) presented a different trend in the ME, particularly for the EoS.

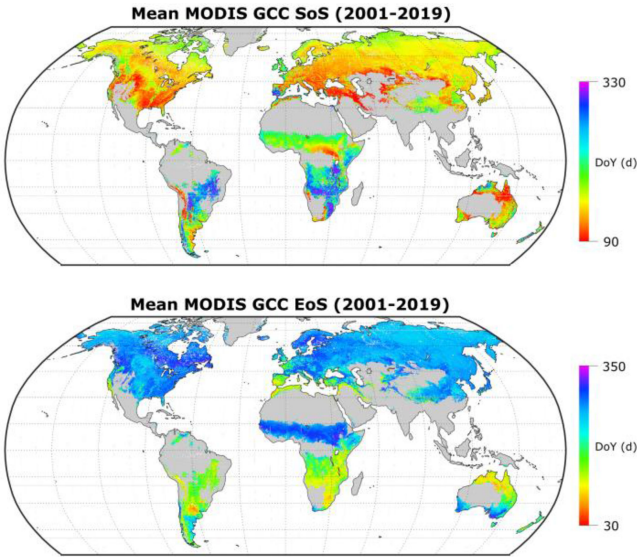

Fig. 4. Maps of the mean start and end of season (SoS and EoS) estimated using the Maximum Separation (MS) method and a dynamic threshold of 50% of the amplitude. The SoS and EoS are shown as the Day of Year (DoY). The MS method was applied to the MODIS Green Chromatic Coordinate Index (GCC) (MOD09GA).

The RMSE between MODIS and PhenoCam LSP metrics depended to a great extent on the type of vegetation. The ME and RMSE differed between land covers in MODIS GCC (see Fig. 3) and the rest of MODIS variables (Fig. 5 of the supplementary material). The best results were found in DBF and MX in the four methods (e.g., ME = 7.2 d and RMSE = 0.6 d for EoS and ME = 0.2 d and RMSE = 12.8 d for EoS in DBF estimated with MS). Contrarily, on average, land covers that represented evergreen showed a high RMSE.

The maps of mean SoS and EoS estimated with MS using the MODIS GCC product for the period 2001–2019 are presented in Fig. 4, and the maps generated with the NDVI, EVI, and LAI are presented in Fig. 6 of the supplementary material. The four vegetation indices showed similar spatial patterns at the global scale.

IV. Discussion

The proposed MS method showed accuracy similar to the best threshold method. Differences in accuracy were higher among land cover types and threshold values rather than LSP methods and MODIS variables. Although MS did not excel in the comparison with PhenoCam, the proposed method presents an advantage over the threshold method; MS was applied directly to daily nonsmoothed time series and with fewer parameters compared to the conventional threshold method with preprocessing steps. The simplicity of the MS method allowed a straightforward implementation in GEE and the production of phenological maps at the global scale. In this way, GEE allowed the rapid processing of custom algorithms and overcame the computing time that would be necessary for processing LSP maps with a local computer.

One of the two parameters of the MS method is the size of the moving window, which can be set with prior knowledge of the length of the growing season. A large window entailed a higher computational cost, but it positively affected the estimation of the phenological metric (see Fig. 3 of the supplementary material), because the window covered more observations and the impact of noise was minimized. The main consideration in the selection of the window size is that it should not exceed the length of the growing season, particularly in vegetation types that present a short growing season such as high-latitude shrublands, alpine GRA, and precipitation-sensitive vegetation.

The second parameter of the MS method is the threshold percentage, which had a strong influence on the accuracy of the LSP estimates (see Fig. 2). The MS, and the threshold methods in general, outputs unreliable LSP estimates when the time series present significant noise and outliers. Noise and outliers may lead to unreliable threshold values in (1), which in turn results in inaccurate LSP estimates. This also explains the good results of the MS and the threshold methods in medium-range threshold percentages (see Fig. 2). For the SoS for instance, a low threshold percentage is more likely to detect a noisy high value as the first observation that overpasses the threshold. These results further prove the robustness of medium threshold percentages against clouds, cloud shadows, and other contamination effects [12], [28].

The MS and the variants of the threshold method performed better in DBF and MX. Deciduous forests generally show a well-defined seasonality that is reflected in sharp changes in the vegetation indices, particularly during the leaf unfolding period. On the contrary, in evergreen, changes in greenness indices are marginal because leaves are perennial, which makes LSP estimation challenging, and phenology changes are observed at the photosynthetic level [30]. Moreover, vegetation indices may not reflect a logistic-type of growth, which explain the poor results of TH3 and a ME that is linearly correlated with the threshold percentage (see Fig. 2). The authors in [20] reported that EVI did not reflect a logistic growth in specific ecosystems and, thus, justified the use of the threshold method for the MODIS Land Cover Dynamics version 6 over the logistic modeling used in the previous version of the product.

V. Conclusion

This study proposed a new method (maximum separation, MS) ideal for fast and large-scale estimates of phenological metrics in cloud-computing platforms such as GEE. The MS presents similar results as the threshold method with time-series preprocessing, but the simplicity of its implementation when applied to different satellite products makes MS more pragmatic than the threshold method, particularly when the data require preprocessing for time series smoothing. We provide the GEE code and Python implementation, which can be used in other remotely sensed data. Future studies may, thus, benefit from this method and customize it for their regional studies.

Appendix

Supplementary Materials are provided with six supplementary figures and three supplementary tables. The Python and JavaScript (Google Earth Engine) implementations of the Maximum Separation (MS) method can be found at https://github.com/adriadescals/MaximumSeparation_method. The Python

code is a demo of the MS method applied to a sample time series, while the JavaScript code is an implementation of the method in Google Earth Engine. The maps estimated with MODIS LAI for 2019 can be visualized at https://adriadescals.users.earthengine.app/view/phenologymslai2019.

REFERENCES

[1] L. Zeng, B. D. Wardlow, D. Xiang, S. Hu, and D. Li, "A review of vegetation phenological metrics extraction using time-series, multispectral satellite data," *Remote Sens. Environ.*, vol. 237, 2020, Art. no. 111511.

[2] E. E. Cleland, I. Chuine, A. Menzel, H. A. Mooney, and M. D. Schwartz, "Shifting plant phenology in response to global change," *Trends Ecol. Evol.*, vol. 22, no. 7, pp. 357–365, Jul. 2007.

[3] J. Peñuelas and I. Filella, "Responses to a warming world," *Science*, vol. 294, no. 5543, pp. 793–795.

[4] C. Körner and D. Basler, "Phenology under global warming," *Science*, vol. 327, no. 5972, pp. 1461–1462, Mar. 2010.

[5] J. Peñuelas and I. Filella, "Phenology feedbacks on climate change," *Science*, vol. 324, no. 5929, pp. 887–888, 2019.

[6] N. Gorelick, M. Hancher, M. Dixon, S. Ilyushchenko, D. Thau, and R. Moore, "Google Earth Engine: Planetary-scale geospatial analysis for everyone," *Remote Sens. Environ.*, vol. 202, pp. 18–27, 2017.

[7] X. Li, Y. Zhou, L. Meng, G. R. Asrar, C. Lu, and Q. Wu, "A dataset of 30 m annual vegetation phenology indicators (1985–2015) in urban areas of the conterminous United States," *Earth Syst. Sci. Data*, vol. 11, pp. 881–894, 2019.

[8] S. van der Walt, S. C. Colbert, and G. Varoquaux, "The NumPy array: A structure for efficient numerical computation," *Comput. Sci. Eng.*, vol. 13, no. 2, pp. 22–30, 2011.

[9] X. Zhang, M. A. Friedl, and C. B. Schaaf, "Global vegetation phenology from moderate resolution imaging spectroradiometer (MODIS): Evaluation of global patterns and comparison with in situ measurements," *J. Geophys. Res. Biogeosci.*, vol. 111, pp. 1–14, 2006.

[10] P. Jonsson and L. Eklundh, "Seasonality extraction by function fitting to time-series of satellite sensor data," *IEEE Trans. Geosci. Remote Sens.*, vol. 40, no. 8, pp. 1824–1832, Aug. 2002.

[11] N. Viovy, O. Arino, and A. Belward, "The best index slope extraction (BISE): A method for reducing noise in NDVI time-series," *Int. J. Remote Sens.*, vol. 13, no. 8, pp. 1585–1590, 1992.

[12] K. Bórnez, A. Descals, A. Verger, and J. Peñuelas, "Land surface phenology from VEGETATION and PROBA-V data. Assessment over deciduous forests," *Int. J. Appl. Earth Obs. Geoinf.*, vol. 84, 2020, Art. no. 101974.

[13] M. Ma and F. Veroustraete, "Reconstructing pathfinder AVHRR land NDVI time-series data for the Northwest of China," *Adv. Space Res.*, vol. 37, no. 4, pp. 835–840, 2006.

[14] J. I. Fisher, J. F. Mustard, and M. A. Vadeboncoeur, "Green leaf phenology at Landsat resolution: Scaling from the field to the satellite," *Remote Sens. Environ.*, vol. 100, no. 2, pp. 265–279, 2006.

[15] P. Beck, P. Jönsson, K.-A. Høgda, S. Karlsen, L. Eklundh, and A. Skidmore, "A ground-validated NDVI dataset for monitoring vegetation dynamics and mapping phenology in Fennoscandia and the Kola peninsula," *Int. J. Remote Sens.*, vol. 28, no. 19, pp. 4311–4330, 2007.

[16] H. Eerens and D. Haesen, "Software for the processing and interpretation of remotely sensed image time series," *User's Manual Version*, 1.5.2, pp. 1–288, Jul. 2017.

[17] B. Tan *et al.*, "An enhanced TIMESAT algorithm for estimating vegetation phenology metrics from MODIS data," *IEEE J. Sel. Topics Appl. Earth Observ. Remote Sens.*, vol. 4, no. 2, pp. 361–371, Jun. 2010

[18] M. A. White, P. E. Thornton, and S. W. Running, "A continental phenology model for monitoring vegetation responses to interannual climatic variability," *Glob. Biogeochem. Cycles*, vol. 11, no. 2, pp. 217–234, 1997.

[19] B. N. Holben, "Characteristics of maximum-value composite images from temporal AVHRR data," *Int. J. Remote Sens.*, vol. 7, no. 11, pp. 1417–1434, 1986.

[20] J. Gray, D. Sulla-Menashe, and M. A. Friedl, User Guide to Collection 6 MODIS Land Cover Dynamics (MCD12Q2) Product, 2019.

[21] J. Chen, P. Jönsson, M. Tamura, Z. Gu, B. Matsushita, and L. Eklundh, "A simple method for reconstructing a high-quality NDVI time-series data set based on the Savitzky–Golay filter," *Remote Sens. Environ.*, vol. 91, no. 3/4, pp. 332–344, 2004.

[22] R. Myneni, Y. Knyazikhin, and T. Park, MCD15A3H MODIS/Terra+ Aqua Leaf Area Index/FPAR 4-day L4 Global 500m SIN Grid V006, Sioux Falls, SD, USA, 2015.

[23] E. Vermote and R. Wolfe, "MOD09GA MODIS/Terra Surface Reflectance Daily L2G Global 1km and 500m SIN Grid V006," distributed by NASA EOSDIS Land Processes DAAC. 2020, Sioux Falls, SD, USA, 2015.

[24] O. Sonnentag *et al.*, "Digital repeat photography for phenological research in forest ecosystems," *Agricultural Forest Meteorol.*, vol. 152, pp. 159–177, Jan. 2012.

[25] Y. Knyazikhin, "MODIS leaf area index (LAI) and fraction of photosynthetically active radiation absorbed by vegetation (FPAR) product (MOD 15) algorithm theoretical basis document," Httpeospso GSFC NASA Govatbdmodistabls Heml, Missoula, MT, USA, 1999.

[26] B. Seyednasrollah *et al.*, "Tracking vegetation phenology across diverse biomes using Version 2.0 of the PhenoCam Dataset," *Sci. Data*, vol. 6, no. 1, pp. 1–11, 2019.

[27] K. Hufkens, M. Friedl, O. Sonnentag, B. H. Braswell, T. Milliman, and A. D. Richardson, "Linking near-surface and satellite remote sensing measurements of deciduous broadleaf forest phenology," *Remote Sens. Environ.*, vol. 117, pp. 307–321, 2012.

[28] D. K. Bolton, J. M. Gray, E. K. Melaas, M. Moon, L. Eklundh, and M. A. Friedl, "Continental-scale land surface phenology from harmonized Landsat 8 and Sentinel-2 imagery," *Remote Sens. Environ.*, vol. 240, 2020, Art. no. 111685.

[29] E. Dinerstein *et al.*, "An ecoregion-based approach to protecting half the terrestrial realm," *BioScience*, vol. 67, no. 6, pp. 534–545, 2017.

[30] G. Yin, A. Verger, I. Filella, A. Descals, and J. Peñuelas, "Divergent estimates of forest photosynthetic phenology using structural and physiological vegetation indices," *Geophys. Res. Lett.*, 2020, Art. no. e2020GL089167.

Adrià Descals received the bachelor's degree in forestry engineering from the Polytechnical University of Valencia, Valencia, Spain, in 2014 and the master's degree in remote sensing from the University of Valencia, Valencia, Spain, in 2016. He is currently working toward the Ph.D. degree in climate-vegetation dynamics with CREAF, Barcelona, Spain.

Aleixandre Verger received the Ph.D. degree in physics from the Universitat de València (UV), Valencia, Spain, in 2008.

He was a Researcher with the Remote Sensing Unit-UV from 2008 to 2010, EMMAH-INRA, Avignon, France, from 2010 to 2013, and has been with the Global Ecology Unit-CREAF, Barcelona, Spain, since 2013. He is currently the Principal Investigator with CREAF of the European Union Copernicus Global Land Service (C-GLOPS1). His main research interests include the development and validation of retrieval algorithms for the estimation of biophysical variables, and climate-vegetation dynamics.

Gaofei Yin received the Ph.D. degree in remote sensing from the Institute of Remote Sensing and Digital Earth, Chinese Academy of Sciences, Beijing, China, in 2015.

From 2015 to 2018, he was with the Institute of Mountain Hazards and Environment, Chinese Academy of Sciences. Since 2018, he has been an Associate Professor with the Faculty of Geosciences and Environmental Engineering, Southwest Jiaotong University, Chengdu, China. He is currently a Marie Skłodowska-Curie Individual Fellow with CREAF, Barcelona, Spain. His current research interests include canopy reflectance modeling, biophysical variables estimation, and climate-vegetation dynamics.

Josep Peñuelas received the Ph.D. degree in ecology from the Universitat de Barcelona, Barcelona, Spain, in 1985.

He is currently a Research Professor with the National Research Council of Spain (CSIC) and the Director of the CREAF-CEAB-CSIC-UAB Global Ecology Unit, Barcelona, Spain. He is a highly cited Scientist ecology/environment, in plant and animal sciences, agricultural sciences, geosciences and in all science fields of the ISI essential science indicators. (h index: 127 GS, i10 index: 653, and more than 81.500 citations GS). He has been a Principal Investigator or Scientific Coordinator of several European Union, Spanish, and Catalan projects financed by public research agencies and by private funding. Among them, he has been awarded with ERC-Synergy 2014–2019 Grant for the IMBALANCE-P project. His recent subjects of study are global change, climate change, atmospheric pollution, biogenic volatile organic compounds emissions, remote sensing, plant ecophysiology, and functioning and structure of terrestrial plants and ecosystems.